Available online at www.sciencedirect.com
ScienceDirect
Geochimica et Cosmochimica Acta 71 (2007) 2960–2974
Geochimica et Cosmochimica Acta
www.elsevier.com/locate/gca

Variability in oceanic dissolved iron is dominated by the colloidal fraction

B.A. Bergquist [a,c,*], J. Wu [b], E.A. Boyle [c]

[a] Department of Geological Sciences, University of Michigan, 2534 C.C. Little Building, 1100 N. University Ave, Ann Arbor, MI 48109, USA
[b] International Arctic Research Center, University of Alaska-Fairbanks, Fairbanks, AK 99775, USA
[c] Earth, Atmospheric, and Planetary Sciences, Massachusetts Institute of Technology, Cambridge, MA 02139, USA

Received 20 September 2006; accepted in revised form 12 March 2007; available online 27 March 2007

Abstract

Oceanic surface and deep iron distribution and size fractionation were investigated on three cruises in the sub-tropical and tropical Atlantic Ocean. Detailed profiles and transects were collected and analyzed for “dissolved” Fe (DFe, 0.4 μm filtered) and “soluble” Fe (SFe, 0.02 μm filtered). The difference between DFe and SFe is inferred to be the “colloidal” fraction of Fe (CFe). SFe concentration distributions and profiles showed little variability in the Atlantic Ocean with slightly lower concentrations of SFe in the upper ocean than the relatively uniform concentrations observed in deep-water (≈0.3 to 0.4 nmol/kg). In contrast, variability in the Atlantic DFe was dominated by variability in CFe. DFe and CFe followed dust deposition trends, and observed surface maxima in DFe profiles were always due to maxima in the CFe fraction. Where dust deposition and surface DFe were low (i.e., the South Atlantic), the CFe fraction of DFe was low and frequently negligible in surface waters. Below the surface maxima in CFe and DFe, CFe always decreased to negligible levels at 30–80 m, remained low or negligible throughout the pycnocline, and increased with depth below the pycnocline. At a site located on the edge of the equatorial system (10°N), high DFe and CFe concentrations were associated with an oxygen minimum zone (OMZ) at depths of 130 to 1100 m. Deep-water DFe and CFe concentrations varied between water masses depending on the source, age, and path of the water masses. DFe in NADW decreased by 30% from the North Atlantic to the South Atlantic site with most of the decrease due to loss of CFe. At the South Atlantic site, NADW had higher DFe and a higher fraction of CFe than the Antarctic water masses.

1. INTRODUCTION

Iron is an essential nutrient for all living organisms. For example, Fe is necessary for chlorophyll production and nitrogen assimilation (Rueter and Ades, 1987). Despite its abundance in the environment, Fe is found at very low concentrations in the ocean due to the low solubility of Fe under oxidizing conditions and is a limiting nutrient for primary productivity in many of regions of the ocean (Martin and Fitzwater, 1988; Martin et al., 1990a,b, 1994; Coale et al., 1996; Hutchins and Bruland, 1998; Boyd et al., 2000, 2004; Coale et al., 2004). It has also been hypothesized that iron could indirectly affect primary productivity in the low nutrient, low chlorophyll regions of the subtropical gyres by limiting nitrogen fixing bacteria, which bring new nitrate into the system (Letelier and Karl, 1996; Michaels et al., 1996; Karl et al., 1997; Falkowski, 1998). These observations and hypotheses have lead to proposals that changes in Fe flux to the ocean may play a role in climate change by influencing oceanic primary production and hence the carbon cycle (Martin et al., 1990a; Kumar et al., 1995; Falkowski, 1998).

The coupling of Fe to the carbon cycle is influenced by its bioavailability, and the bioavailability of Fe influenced

---

[*] Corresponding author. Address: Department of Geological Sciences, University of Michigan, 2534 C.C. Little Building, 1100 N. University Ave, Ann Arbor, MI 48109, USA. Fax: +1 734 763 4690.

E-mail address: bbergqui@umich.edu (B.A. Bergquist).

0016-7037/$ - see front matter © 2007 Elsevier Ltd. All rights reserved.
doi:10.1016/j.gca.2007.03.013

by its physicochemical speciation (Barbeau and Moffett, 1998; Hutchins et al., 1999; Nordwell and Price, 2001; Chen et al., 2003). In recent years, two important observations of Fe speciation in the ocean have been made: (1) >99% of dissolved Fe (DFe, <0.4 μm) is complexed by organic ligands in the ocean (Gledhill and van den Berg, 1994; Rue and Bruland, 1995; Wu and Luther, 1995; Luther and Wu, 1997; Witter and Luther, 1998; Powell and Donat, 2001), and (2) a significant fraction of dissolved Fe (30–70% in deep-water) in the ocean is present as colloids, small particles that pass through 0.4 and 0.2 μm filters (Wu et al., 2001). Dissolved organic ligands appear to be ubiquitous in the ocean and are usually found in excess (≈0.5 to 2 nmol/kg) of DFe concentrations (Gledhill and van den Berg, 1994; Rue and Bruland, 1995; Wu and Luther, 1995; Witter and Luther, 1998; Powell and Donat, 2001). Thus, organic ligands likely enhance the residence time and solubility of DFe in the ocean.

Significantly less work has been done on the distribution and importance of colloidal Fe in the ocean. Wu et al. (2001) found that the colloidal fraction (CFe, 0.02–0.4 μm) and soluble fraction (SFe, <0.02 μm) of DFe had different concentration profiles suggesting unique biogeochemical behaviors for the two pools of Fe. The different behaviors of colloidal and soluble Fe have yet to be rigorously studied along with the potential biological consequences that a significant fraction of the DFe in the ocean is colloidal. There is evidence that marine organisms can utilize colloidal Fe, although growth rates are usually slower than organisms grown on free Fe (Barbeau and Moffett, 1998; Nordwell and Price, 2001; Chen et al., 2003). Only a few studies have investigated the role of organic ligands in determining the distribution between SFe and CFe. In general excess organic ligands have been found to be both in the soluble and colloidal size fractions (Wu et al., 2001; Cullen et al., 2006), but the role that organic ligands play in establishing the distribution between colloidal and soluble Fe is not well understood. In order to assess the role of colloidal Fe in the cycling of Fe in the ocean, we need to study the distribution, biogeochemical cycling, and biological utilization of both colloidal and soluble Fe and understand how these two pools interact.

The aim of this study was to investigate oceanic Fe distribution and size fractionation in areas of varying atmospheric dust inputs in the Atlantic Ocean. We present data from three cruises in the sub-tropical and tropical Atlantic Ocean (30°N–30°S) including both surface data and profiles of Fe including high-density profiles in the upper 200 m (Fig. 1). Iron concentrations were measured by a new isotope dilution multi-collector inductively coupled plasma mass spectrometry (MC-ICPMS) method (Bergquist, 2004; Bergquist and Boyle, 2006).

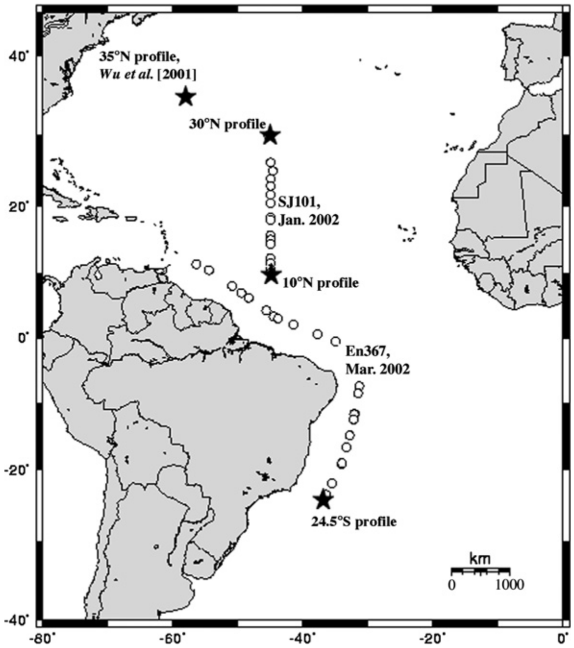

Fig. 1. Sample location map for the three cruises discussed in this study. Surface samples are marked by circles, and profile sites are marked with their latitude and stars. The northwest Atlantic profile site from Wu et al. (2001) is also shown.

2. SAMPLING AND METHODS

2.1. Sampling sites

Between January 2001 and March 2002, trace metal clean seawater samples were collected on three cruises in the sub-tropical and tropical Atlantic Ocean (Fig. 1): (1) January 2001 (R/V Seward Johnson, SJ0101, surface sampling and deep profiles), (2) June/July 2001 (R/V Knorr, Knr162, surface sampling and detailed euphotic zone profiles), (3) March 2002 (R/V Endeavor, En367, surface sampling, detailed euphotic zone and deep profiles). The two 2001 cruises focused on the North Atlantic sub-tropical and tropical regions and were part of the NSF-sponsored Biocomplexity MANTRA program in which sampling sites were chosen based on variations in dust input and possible connections with N_2 fixation. Two sites were visited in both the winter and summer of 2001 (30°N, 45°W and 10°N, 45°W), which allowed for sampling at both times of year in the upper 200 m. The northern site at 30°N is in the subtropical gyre and is characterized by oligotrophic conditions, a deep pycnocline, and lower atmospheric dust inputs than the 10°N site. The 10°N site is on the edge of the subtropical gyre and equatorial system and has a shallow pycnocline and higher atmospheric dust inputs. The March 2002 cruise followed along the western part of the Atlantic basin from Barbados to Rio de Janeiro, Brazil. The deep South Atlantic profile presented in this study was taken at the southernmost extent of the cruise (24.5°S, 37°W) in the subtropical gyre of the South Atlantic. The sampling sites cover an area in the Atlantic where estimated dust deposition rates vary by orders of magnitude both from north to south and seasonally (Duce and Tindale, 1991; Fung et al., 2000; Gao et al., 2001; Vink and Measures, 2001; Chen and Siefert, 2004). Dust deposition rates are highest in the North Atlantic downwind from the Sahara and decrease rapidly south of the inter-tropical convergence zone (ITZC).

2.2. Sampling methods

The trace metal clean seawater samples collected in this study were collected using a variety of methods. Many of the samples collected on the cruise were taken with the Moored In situ Trace Element Serial Sampler (MITESS) water sampler or with a single MITESS "ATE" (Automated Trace Element) module (Bell et al., 2002). Each MITESS module opens and closes an acid-cleaned 500 ml polyethylene bottle while underwater in order to minimize chances for contamination. Near surface samples were collected by (a) "ATE/Vane", a single MITESS module attached to a "weather-vane" that is free to rotate around the hydrowire and orients itself such that the module is upstream of the wire while ship moves forward at 1–2 knots placing the sampler upstream of the wire and wire contamination, (b) an underway "towed fish" device (Vink et al., 2000) deployed while the ship is steaming up to ≈10 knots or (c) "pole" sampling, extending a sample bottle from the side of a ship using a long pole while the ship is moving forward at 1–2 knots. Profile samples were collected using either the "ATE/Vane" device with a single MITESS module for shallow samples (<200 m) or the full 12 unit MITESS for deeper samples (>30 m). Details of the different type of sampling schemes can be found in Bergquist (2004), Boyle et al. (2005), and Bergquist and Boyle (2006).

After sample collection, sealed sample bottles were taken into a class 100 clean air flow environment for filtration within 12–24 h of collection in order to avoid Fe loss to bottle walls. Splits of each sample were vacuum filtered through acid cleaned 0.4 μm Nuclepore® filters and syringe filtered though acid cleaned 0.02 μm Anotop® alumina filters (details of 0.02 μm filtration in Wu et al., 2001). For the 0.4 μm filter step, acid cleaned filters and the filter rig were thoroughly rinsed with dilute trace metal clean HCl (≈0.01 M) and then several aliquots of seawater prior to filtration. For the 0.02 μm filtration, the 0.02 μm Anotop® alumina syringe filters were cleaned by passing three 10 ml aliquots of dilute trace metal clean HCl (≈0.01 M) through the syringe filter using an acid cleaned high-density polyethylene syringe (o-ring free) immediately followed by rinsing with trace metal clean water until the pH was ≈5.5 (to avoid compromising the alumina filter material). Three 10 ml aliquots of seawater were then passed through the 0.02 μm syringe filters before collection of the filtrate for SFe analysis. The acid cleaned collection bottles for both the 0.4 and 0.02 μm filtrates were also rinsed several times with filtered seawater prior to the final sample collection. Two to three separate aliquots of the filtrates were collected and the sequence noted on bottles. The last aliquot is the sample usually measured for Fe concentration because it is considered to be least likely to have been contaminated during filtration. Filtrates were acidified at sea in a class 100 clean environment to pH 2 by addition of triply distilled Vycor 6 N HCl in a ratio of 1 ml acid to 500 ml of seawater.

2.3. Fe concentration measurement

Iron concentrations on filtrates were measured by a modified version of the method by Wu and Boyle (1998), which utilizes isotope dilution followed by $Mg(OH)_2$ co-precipitation and measurement by ICPMS (Bergquist, 2004; Bergquist and Boyle, 2006). The main differences of the technique used in this study are the use of a ^{54}Fe isotope spike and a GV Instruments (formerly Micromass) IsoProbe MC-ICPMS. The IsoProbe incorporates a hexapole collision cell prior to the magnet that eliminates $^{40}Ar^{16}O^+$ and $^{40}Ar^{14}N^+$ interferences on masses 56 and 54, which allows samples to be measured in low mass resolution. The multi-collection feature permits simultaneous collection of masses 52 (monitor Cr and correct for Cr interference on ^{54}Fe), 54, 55 (Mn), 56, and 57. Mn and Cr data are discussed in Bergquist (2004). The largest interference correction for Fe is CaO^+ on mass 56. The CaO^+ interference is monitored by measuring $CaOH^+$ on mass 57, measuring the CaO/CaOH ratio on a trace metal clean Ca solution throughout the run, and correcting mass 56 for the CaO^+ interference. Details of the method can be found in Bergquist (2004) and Bergquist and Boyle (2006). Briefly, replicate analysis of samples yield precisions of better than ±0.05 nmol/kg for Fe. Error bars reported in this study represent the 1σ standard deviation (SD) of replicate analysis of samples. Procedural blanks for Fe ranged from 0.08 to 0.17 nmol/kg with a typical precision of ±0.03 nmol/kg (1σ SD) for an individual analytical session.

3. RESULTS AND DISCUSSION

3.1. Surface distribution

The surface distributions of DFe and SFe from 30°N to 25°S are shown in Fig. 2. DFe and CFe values are highest in the North Atlantic (0.6 and 0.3 nmol/kg, respectively) and decrease significantly south of the equator (0.3 and <0.1 nmol/kg, respectively). In contrast, the mean SFe concentration is similar for both the North Atlantic (0.32 ± 0.11 nmol/kg, $n = 12$) and South Atlantic (0.28 ± 0.05 nmol/kg, $n = 9$). In general the observed trends in DFe and CFe are similar to trends of other dust derived trace metals (e.g., Al and Mn) (Vink and Measures, 2001; Bergquist and Boyle, 2006), and both the DFe and CFe transect data show maxima in the North Atlantic near 20°N in the zone of maximum dust transport off of Africa (Prospero, 1996; Mahowald et al., 1999; Fung et al., 2000; Gao et al., 2001; Gregg et al., 2003; Bergquist and Boyle, 2006).

Because most of the N–S variation is observed in the DFe and not in the SFe fraction, much of the structure observed in the DFe transect is due to CFe. Wu et al. (2001) suggested that most atmospherically derived DFe was preferentially released into the colloidal pool. This assumption was based on profiles from oligotrophic gyre sites in the North Atlantic and North Pacific where surface maxima in the DFe were observed without corresponding maxima SFe. Our surface CFe and SFe distributions support that interpretation; CFe follows the dust deposition variations and the Al distribution from Vink and Measures (2001). In the southern part of the transect where dust deposition is the lowest, the colloidal fraction of DFe disappears and then increases slightly at the southernmost

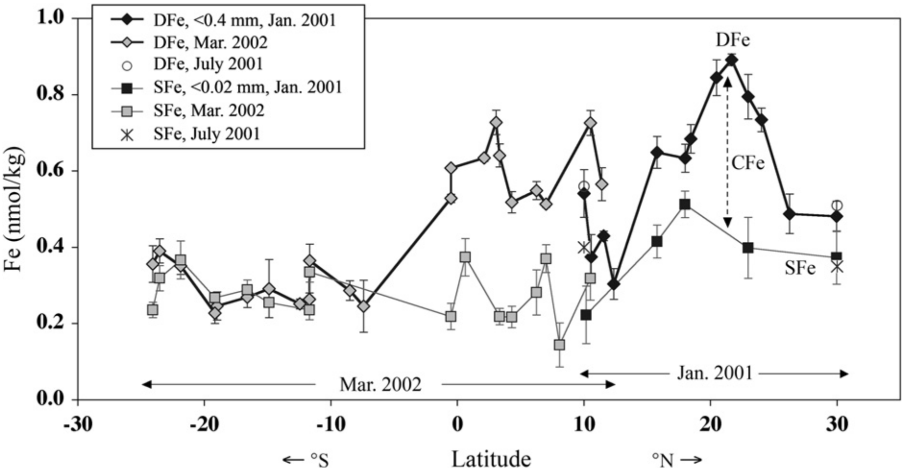

Fig. 2. DFe and SFe surface data along a N–S transect from 30°N to 30°S in the western Atlantic. Transects from the January 2001 and March 2002 cruises were combined and are marked by a break in the transect. DFe and SFe data for the stations re-sampled on the summer, 2001, cruise are also shown (30°N and 10°N). Error bars are 1σ standard deviation of sample replicates (external reproducibility is typically less than ±0.05 nmol/kg (1 SD)).

station where DFe and Al also start to increase again. It is interesting that SFe does not show as strong of a trend from north to south as CFe, although a few higher concentration values of SFe (>0.4 nmol/kg) exist under the zone of maximum transport of Saharan dust (≈20°N). This observation implies that the SFe distribution is not as directly influenced by dust inputs as the CFe fraction.

In Bergquist and Boyle (2006), surface residence time estimates for DFe were made at the profile sites where reasonable assumptions of steady-state could be made. Estimates of surface residence times in the North Atlantic were 1.5–5 months (±50%) using integrated DFe values over the depth of the mixed layer and concurrently measured labile Fe deposition estimates (leachable at pH 4.5) for the input flux (Chen and Siefert, 2004). For the 24.5°S station, concurrent measurements of dust deposition were not available and estimates of dust deposition from Vink and Measures (2001) were used from a similar transect in June 1996. Using a similar percentage of dust solubilization as observed by Chen and Siefert (2004) for the North Atlantic (3%), a surface residence time of 14 months was estimated for DFe at the South Atlantic site. The only way to reduce the surface residence time estimate to a few months using our calculation method is to assume a larger dissolution of atmospheric dust (>10%) or include another significant source of DFe to the mixed layer. Another likely possibility is that DFe surface residence times are longer in regions of the ocean without a large atmospheric input and where the CFe fraction of the DFe is low to negligible.

3.2. Water column profiles

Fig. 3 through 6 show the water column profiles of DFe and SFe at three sites along the N–S transect: (1) 30°N, 45°W, (2) 10°N, 45°W, and (3) 24.5°S, 36°W. DFe and SFe profiles from a station near the Bermuda Rise (35°N, 58°W) from Wu et al. (2001) are shown for comparison in Fig. 5. The 30°N and 10°N stations were sampled both on the January and the July cruises with the deep-water profiles collected in the winter (Fig. 3a and c) and the high-density euphotic zone profiles collected in the summer (Fig. 3b and d). The South Atlantic site was sampled on the March 2002 cruise (Fig. 4b). Table 1 and Appendix B summarize the data from the profiles.

The DFe concentration profiles generally have nutrient-type profiles with lower concentrations in the upper water column than in deep-water, although the profiles have interesting features deviating from classic nutrient-type profiles with surface maxima, intermediate water minima and maxima, and variations clearly associated with water masses. Also, the different pools of DFe (CFe and SFe) have distinct vertical profiles and distributions. Profiles will be discussed in terms of their upper and deep-water column profiles.

3.2.1. *Upper (surface to ≈1000 m) water column Fe profiles*

The two subtropical gyre sites (30°N, Fig. 3a and b, and 24.5°S, Fig. 4a and b) along with the profile from Wu et al. (2001) near Bermuda (Fig. 5a) have very different upper water column profiles of Fe compared with the 10°N site (Fig. 3c and d). The pycnocline extends deeper at the gyre sites (≈750 m), whereas the pycnocline at 10°N is much shallower (<250 m). At all three gyre sites, surface maxima in DFe are observed followed by broad minima in the pycnocline before DFe increases below depths greater than 600 m (Fig. 5a). At the 10°N station (on the edge of the equatorial system), a surface maximum in DFe is observed in the summer and not in the winter (Fig. 3c and d). DFe values increase dramatically at this site to values >1 nmol/kg below the mixed layer and remain high to a depth of 1050 m before decreasing to an average of 0.73 nmol/kg in deep water.

One of the most striking features of the upper ocean profiles is the different vertical distributions of DFe and SFe suggesting distinct biogeochemical behaviors for the SFe and CFe pools. At all sites with surface maxima in DFe, the surface maxima are due to CFe. This is shown in

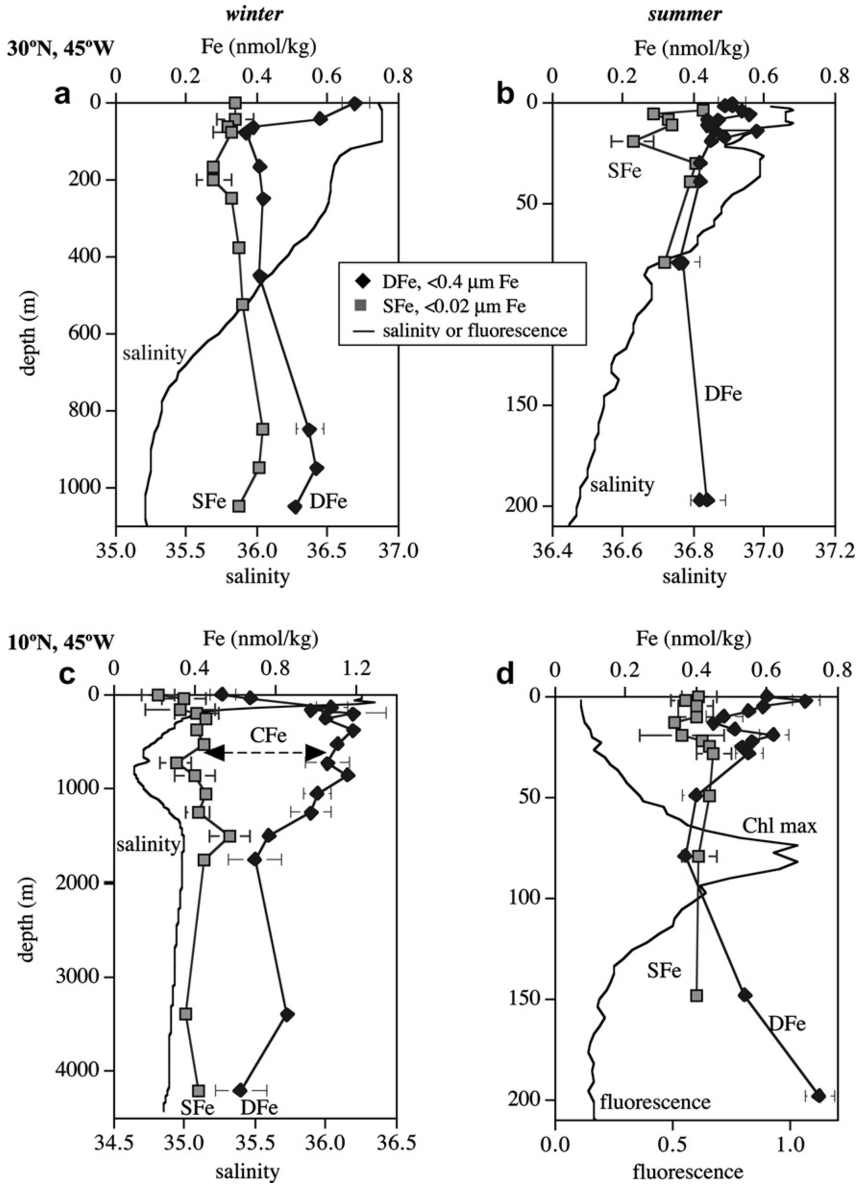

Fig. 3. DFe and SFe water column data at the 30°N, 45°W and 10°N, 45°W stations from both the winter and summer cruises, 2001. (a) The winter 30°N station is plotted with salinity (salinity is reported on the practical salinity unit scale). (b) The summer 30°N station is plotted with salinity. (c) The winter 10°N station is plotted with salinity. (d) The summer 10°N station is plotted with chlorophyll fluorescence. Error bars are 1σ standard deviation of sample replicates (external reproducibility is typically less than ±0.05 nmol/kg (1 SD)).

Fig. 5c and d where maxima are observed in the CFe profiles, but not in the SFe profiles. A pronounced surface maximum in CFe was observed at the 30°N site in the winter (Fig. 3a). CFe decreased within the mixed layer to negligible amounts (0.04 ± 0.05 nmol/kg) by 77 m. The disappearance of CFe was observed at all sites with minima at depths of 30–80 m (Fig. 5d). At depths greater than the minima, CFe values increased to 30% of the DFe pool at 150 m at the 30°N station in the winter and the 10°N station in the summer. In contrast, the CFe pool remained negligible throughout the pycnocline to depths greater than 550 m at the South Atlantic site (Fig. 4b). The northwestern Atlantic site at 35°N sampled by Wu et al. (2001) may be similar to the South Atlantic site in that the CFe is also negligible at 400 and 500 m (Fig. 5d). In general, the SFe profiles show much less structure than the CFe profiles indicating that most of the structure in the DFe profiles is due to CFe.

High sample density profiles in the upper 200 m were collected at the North Atlantic sites in the summer of 2001 (Fig. 3b and d). The goal of this sampling protocol was to examine the upper water column Fe pools in more detail. At both sites, CFe had a surface maximum and decreased to negligible amounts at 30–50 m. The DFe and SFe for the 30°N site are plotted with salinity in Fig. 3b. The mixed layer was very shallow at the time of sampling (11 m) and distinct salinity features in the upper 30 m are present. The DFe and SFe profiles show similar patterns

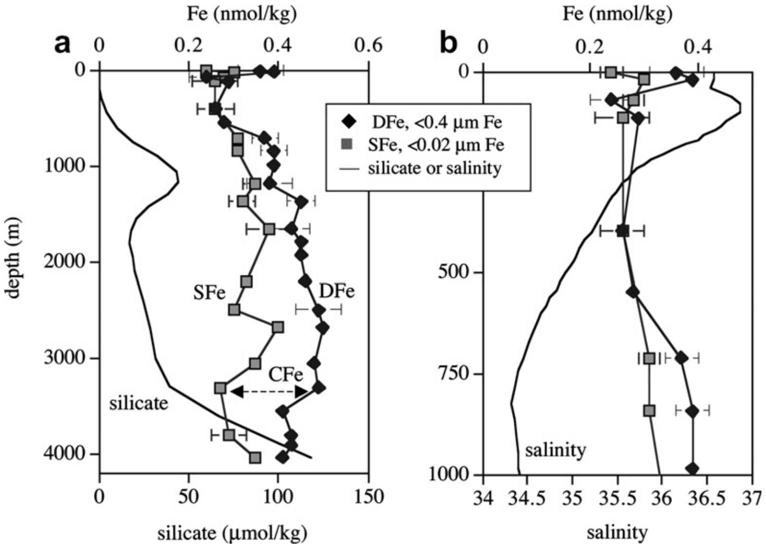

Fig. 4. DFe and SFe profiles for the South Atlantic station at 24.5°S, 37°W occupied in March 2002. (a) Full Fe profile to 4000 m plotted along with silicate data measured on the same cruise. (b) Blow up of the upper 1000 m plotted along with salinity data (salinity is reported on the practical salinity unit scale). Error bars are 1σ standard deviation of sample replicates (external reproducibility typically less than ±0.05 nmol/kg (1 SD)).

Table 1
Summary of water columm Fe data

Depth (m)	DFe (nmol/kg)	1 SD[a]	n[b]	SFe (nmol/kg)	1 SD[a]	n[b]	CFe (nmol/kg)	1 SD[a]	n[b]	CFe/DFe (%)
35°N, 58°W (Wu et al., 2001)										
Mixed layer, <20 m	0.57		1	0.12		1	0.46		1	81
Pycnocline, 50–500 m	0.24	0.05	6	0.24	0.04	2	0.01	0.01	2	0
Deep, >1500 m	0.64	0.05	6	0.32	0.01	4	0.32	0.09	3	50
30°N, 45°W										
Winter mixed layer, 0–100 m	0.51	0.15	4	0.33	0.01	4	0.17	0.17	4	34
Winter mixed layer peak, 0 m	0.68		1	0.34		1	0.34		1	50
Summer mixed layer, 0–11 m	0.50	0.05	8	0.35	0.06	4	0.16	0.08	4	32
Pycnocline, 165–525 m	0.41	0.02	3	0.32	0.03	5	0.11	0.03	2	27
Deep, 850–1050 m	0.54	0.03	3	0.39	0.04	3	0.15	0.02	3	28
10°N, 45°W										
Winter mixed layer, 0–55 m	0.59	0.13	2	0.28	0.10	2	0.31	0.03	2	53
Summer mixed layer, 0–32 m	0.56	0.07	11	0.40	0.04	9	0.17	0.09	9	30
O_2 minimum, 150–1050 m	1.09	0.08	9	0.40	0.06	8	0.61	0.08	8	63
Deep, 1600–4200 m	0.73	0.12	3	0.41	0.05	3	0.31	0.07	3	42
24.5°S, 36°W										
Mixed layer, 0–52 m	0.37	0.03	2	0.27	0.04	2	0.11	0.02	2	30
Pycnocline, 60–550 m	0.27	0.02	4	0.27	0.01	3	0.01	0.02	3	0
AAIW, 700–1200 m	0.38	0.01	4	0.32	0.03	3	0.06	0.03	3	16
NADW, 1700–3350 m	0.47	0.02	7	0.33	0.05	4	0.15	0.05	4	32
AABW/LCPDW, >3500 m	0.42	0.01	4	0.32	0.04	2	0.10	0.05	2	24

[a] 1σ standard deviation of depths used in sample grouping (not the same as analysis replicates).

[b] Number of depths used in sample grouping.

to the salinity profile suggesting that the Fe values are correlated with shallow water mass properties. A similar correlation was observed along a transect in the Sargasso Sea for DFe and temperature (Wu and Boyle, 2002) and in the eastern Atlantic for Al and salinity (Measures, 1995). Although the residence time of Fe in surface waters is probably less than a year, it must be sufficiently long enough that young, shallow water masses retain a memory of their original surface Fe conditions. The same station in the winter was characterized by a deep mixed layer of 100 m; CFe concentrations exhibited a surface maximum and decreased to negligible levels within the mixed layer. This observation

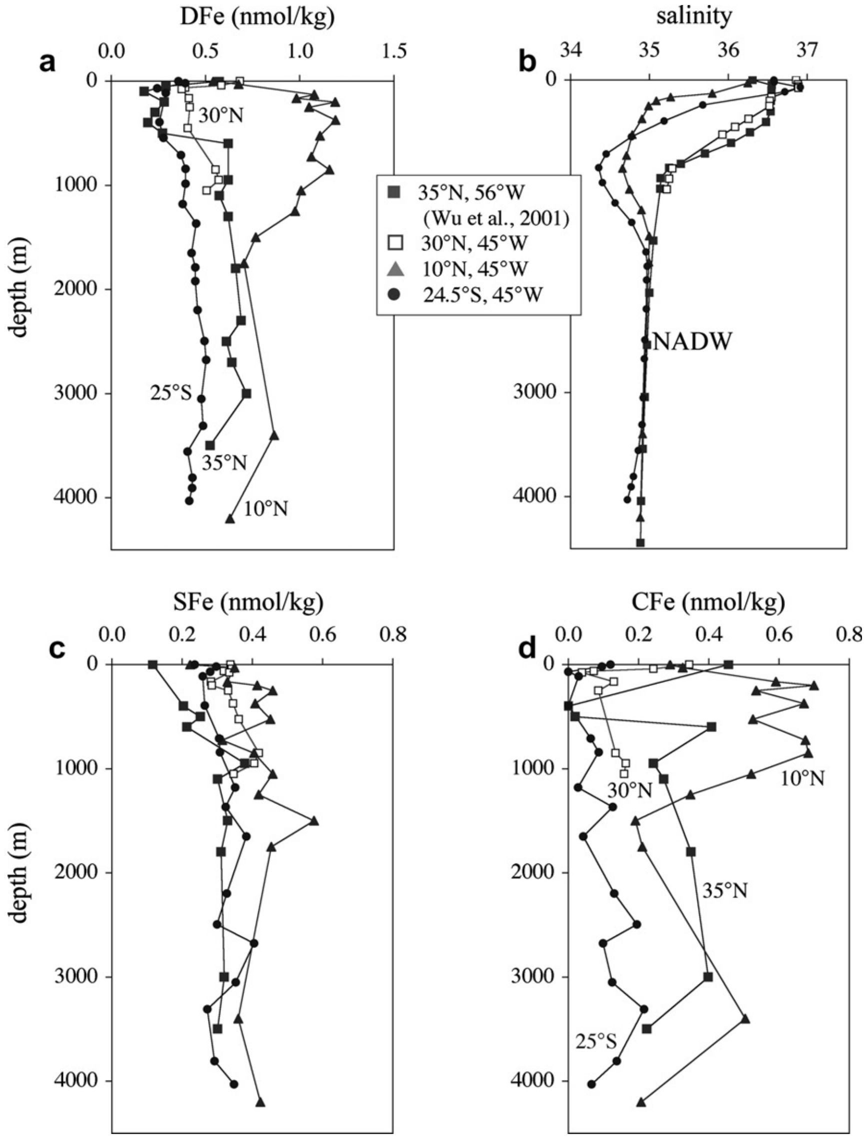

Fig. 5. Fe water column data for the three deep stations sampled in this study (30°N, 45°W; 10°N, 45°W; 24.5°N, 36°W) along with a station sampled near the Bermuda Rise from Wu et al. (2001) (35°N, 56°W). The DFe (<0.4 μm Fe) profiles are shown in (a), the salinity in (b) (salinity is reported on the practical salinity unit scale), the SFe (<0.02 μm Fe) profiles in (c), and the CFe (0.02–0.4 μm) profiles in (d). In (b), the core of North Atlantic Deep Water (NADW) is marked.

contrasts with the summer profile implying that the residence time of CFe is less than the mixing time of the mixed layer during the winter. The winter surface maximum in CFe may be due to a dust deposition event prior to our sampling, as very low atmospheric dust concentrations were measured concurrently at the station (Chen and Siefert, 2004). The 30°N station in the winter is also where a large fraction of labile Fe was measured in the aerosol Fe with a possible anthropogenic source (Chen and Siefert, 2004).

The summer high-density profile at the 10°N station is plotted along with chlorophyll fluorescence in Fig. 3d. The mixed layer depth at the time of sampling was 32 m. The SFe profile shows little variation over the entire depth profile to 150 m (0.40 ± 0.03 nmol/kg, 1 SD), whereas the CFe exhibits a surface maximum and variability within the mixed layer, disappears from 50 to 100 m, and increases with depth to 200 m. The same station in the winter was characterized by a deeper mixed layer (55 m). The DFe concentration increased with depth with most of the increase in the CFe pool in the upper 200 m (Fig. 3c). This station only had 5 depths sampled in the upper 200 m and may have not sampled a CFe minimum, but likely a DFe and CFe minimum did not occur at this time of year due to winter vertical mixing of deeper high DFe waters into the mixed layer. DFe values increased to high levels at shallower depths in the winter than in the summer reaching levels of 1 nmol/kg at 130 m versus 0.54 nmol/kg at 148 m in the summer (Fig. 3c and d).

Below the depth where CFe and DFe minima occur (30–70 m), DFe and CFe concentrations do not increase much in the deep pycnoclines of the subtropical gyre sites (Fig. 5a). DFe values reach very low concentrations (<0.3 nmol/kg) with no CFe present in the pycnocline at both the South Atlantic site (Figure 2.6b) and the 35°N site near Bermuda (Wu et al., 2001). The DFe minimum at the 30°N station remains low throughout the pycnocline as well, but DFe concentrations are higher (0.41 nmol/kg) than the other gyre sites with 27% of the DFe present as CFe. The pycnocline water in the subtropical gyres is formed at higher latitudes (40°N) in the gyres and spreads along isopycnals (Tchernia, 1980). This higher latitude source water is general characterized by lower dust deposition and hence potentially lower surface DFe. In particular in the South Atlantic, this water forms in an area of very low dust deposition. Therefore, the pycnocline waters at the 24.5°S station are likely ventilated by water that sinks with very low DFe and negligible CFe. The reason for the difference between the pycnocline waters of the station near Bermuda (35°N, 65°W) and the 30°N station from this study is less clear (Fig. 5a), but may reflect differences in the sources of the pycnocline water.

The station at 10°N is different from the gyre stations in that the pycnocline is very shallow and high levels of DFe are observed in the upper 1000 m. The zone of high Fe concentration persists from 130 to 1050 m with an average DFe of 1.09 ± 0.08 nmol/kg (1 SD, $n = 9$) with 60% of the DFe present as CFe. The DFe and CFe maxima are associated with an oxygen minimum zone (OMZ) (Fig. 6). The OMZ in the tropical Atlantic is due to enhanced re-mineralization of organic matter sinking (from the high productivity equatorial region) into a slowly ventilating water mass (Siedler and Onken, 1996; Brea et al., 2004; Stramma et al., 2005). More of the DFe in the OMZ is CFe suggesting that re-mineralization of organic matter may preferentially release Fe into the colloidal fraction.

Although surface maxima with subsequent minima in DFe have been measured before (Bruland et al., 1994; Wu et al., 2001), only the Wu et al. (2001) study measured CFe and SFe and observed the CFe pool disappearing completely. Our study is the first to measure DFe, SFe, and CFe in the upper water column at sufficiently high sample density to document the disappearance of the CFe at multiple stations. There are two possible explanations for the disappearance of CFe: (1) transient atmospheric dust deposition and downward mixing with lower DFe and CFe water and/or (2) some removal mechanism for the CFe between ≈30 and 80 m. There are several possible removal mechanisms for CFe: (1) colloidal aggregation and settling, (2) dissociation of colloidal ligand complexes and subsequent uptake by organisms or scavenging onto particles, and (3) direct use of colloidal Fe by organisms (i.e., ingestion). There is evidence that marine organisms can grow utilizing colloidal Fe, although growth rates are usually lower than organisms grown on free Fe (Barbeau et al., 1996; Barbeau and Moffett, 1998, 2000; Chen and Wang, 2001; Nordwell and Price, 2001; Chen et al., 2003). However, with our data it is impossible to distinguish a biological removal mechanism from a scavenging/aggregation removal term at a similar depth. The reappearance of CFe in deeper waters does suggest that CFe is regenerated at depth through re-mineralization of organic matter.

3.2.2. *Deep-water column Fe profiles*

Two deep-water profiles were collected at 10°N and 30°N during the winter 2001 North Atlantic cruise and one deep profile was sampled at 24.5°S on the March 2002 South Atlantic cruise. The 10°N station profile was sampled to 4200 m. Below the high DFe of the OMZ, DFe values decrease to an average value of 0.73 ± 0.12 nmol/kg (1 SD, $n = 3$) below 1600 m (Figs. 3c and Fig. 6). The decrease in the DFe concentration is entirely due to a decrease in the fraction of CFe from ≈60% of the DFe in the OMZ to 40% at depths greater than 1600 m. SFe concentrations do not change with depth throughout the OMZ and deeper at this site. From the salinity profile (Fig. 5b), the water from 1600 to 4200 m can be identified as North Atlantic Deep Water (NADW). The Wu et al. (2001) 35°N station also sampled NADW

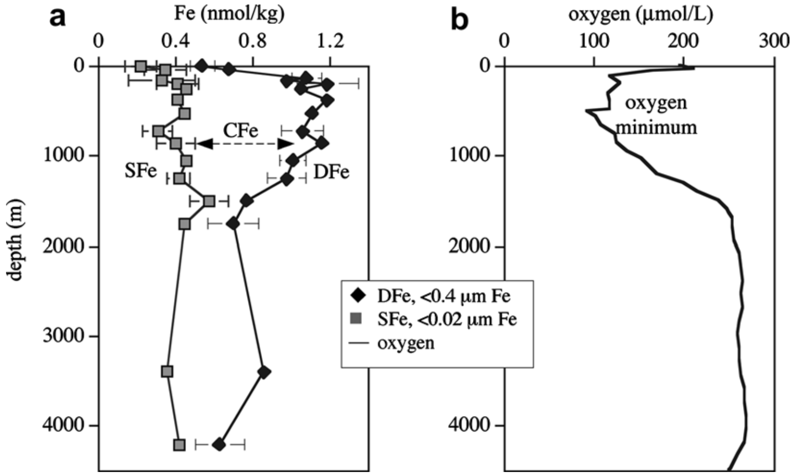

Fig. 6. (a) DFe and SFe from the winter 10°N, 45°W station. Error bars are 1σ standard deviation of sample replicates (external reproducibility is typically less than ±0.05 nmol/kg (1 SD)). (b) Dissolved oxygen data from the nearby GEOSECS station 39 (7.8°N, 43.9°W). Temperature and salinity overlays for our station and the GEOSECS station were nearly identical.

(see salinity profile, Fig. 5b) and had an average value of 0.64 ± 0.05 nmol/kg ($n = 6$) at depths greater than 1600 m (Fig. 5a), which is lower than our observed value. However, we only have three samples below 1600 m and the 3400 m sample yielded high concentrations (0.86 nmol/kg) and hence is potentially contaminated. The concentration was measured in analyses from both filtrate bottles, so the datum is retained in the sample plots and calculations. Without the 3400 m point, the 10°N NADW average for DFe would be 0.67 ± 0.05 nmol/kg ($n = 2$) and is indistinguishable from the Wu et al. (2001) 35°N NADW value. The 30°N station was only sampled to 1050 m and did not sample NADW, but both DFe and SFe concentrations increase below the pycnocline (Fig. 3a).

The South Atlantic water column profile Fe data are the first reported for both DFe and SFe for this region of the ocean. In Fig. 4a, the DFe and SFe profiles are shown along with reactive silicate data. Antarctic Intermediate Water (AAIW) is the high-Si water just below the pycnocline from 700 to 1200 m and has a DFe value of 0.38 ± 0.01 nmol/kg (1 SD, $n = 4$). NADW has lower Si concentration and forms the core of the deep water from 1700 to 3350 m with higher DFe concentrations (0.47 ± 0.02 nmol/kg, 1SD, $n = 7$). Below 3500 m, Si levels increase to very high levels at 4040 m (118 μmol/kg) indicative of Antarctic Bottom Water/Lower Circumpolar Deep Water (AABW/LCPDW). The DFe in the AABW was 0.42 ± 0.01 nmol/kg (1 SD, $n = 4$). Our DFe concentrations in the Antarctic derived water masses agree well with DFe measured in the Atlantic sector of the Southern Ocean. Surface waters vary from 0.1 to 0.5 nmol/kg (Martin et al., 1990a; de Baar et al., 1995; Loscher et al., 1997), and DFe concentrations from a profile near the Drake Passage were 0.10–0.16 nmol/kg at the surface and increased to 0.40 nmol/kg at 550 m (Martin et al., 1990a).

All of the structure in the observed deep-water DFe profile at 24.5°S and in most of the DFe data in this study is due to CFe (Fig. 5c, d, and 7). The SFe at the South Atlantic site is invariant at depths greater than 700 m (0.33 ± 0.04 nmol/kg, 1 SD, $n = 12$). The average value of deep-water SFe from the North Atlantic sites (0.38 ± 0.08 nmol/kg, 1 SD, $n = 14$) is only slightly higher than the deep-water SFe at the South Atlantic site. In contrast, the deep-water CFe decreases from 0.26 ± 0.11 nmol/kg (1 SD, $n = 13$) in the North Atlantic to 0.11 ± 0.06 nmol/kg (1 SD, $n = 12$) in the South Atlantic. The difference is significant at the 95% confidence level using both the *t*-test and a distribution-free test, the Kolmogorov–Smirnov test (Hollander and Wolfe, 1973). If one looks only at the NADW, the CFe fraction decreases from 40 to 50% of the DFe in the North Atlantic to 30% at the South Atlantic site. This loss in CFe along the transit path suggests that CFe is preferentially lost along the flow path of this water. Despite having lower CFe concentrations than further north, the NADW at 24.5°S still has a larger fraction of CFe than the Antarctic water masses. The CFe fraction of the DFe is slightly lower in the AAIW and AABW/LCPDW (≈20% of DFe) compared to the NADW (≈30% of DFe) at the South Atlantic site. This difference between the NADW and the Antarctic derived water masses is likely due to high dust input and regeneration of Fe-replete sinking organic matter in the North Atlantic compared to the very low initial Fe concentrations of Antarctic surface waters.

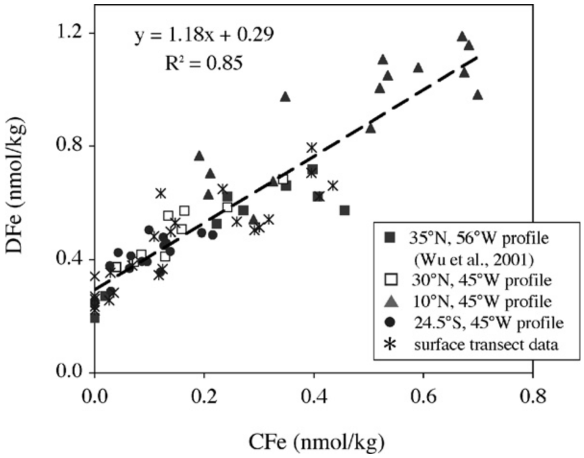

Fig. 7. CFe plotted against DFe. This plot illustrates that most of the structure observed in the DFe data is due to variations in CFe, especially at DFe concentrations above 0.3 nmol/kg.

3.2.3. Deep water scavenging residence time

A scavenging residence time for DFe (270 ± 140 years) in the NADW was estimated from the difference between DFe in the North Atlantic sites and the South Atlantic site in Bergquist and Boyle (2006). In order to calculate a scavenging residence time for the DFe in the NADW, several factors were considered including (1) dilution of the NADW with low Fe Antarctic water, (2) re-mineralization of organic bound Fe along the flow path, and (3) the transit time of NADW from the North Atlantic (at 10°N) to the South Atlantic site (24.5°S). It was found that the estimate was most sensitive to the decrease in DFe and the assumed transit time. The NADW at the South Atlantic site (0.47 ± 0.02 nmol/kg, 1 SD, $n = 4$) has significantly less DFe than the average of NADW from the northern sites (0.67 ± 0.09 nmol/kg, 1 SD, $n = 9$). Again, most of the decrease from the North Atlantic to the South Atlantic site in the DFe pool occurs in the CFe pool. The average SFe for the North Atlantic NADW (0.36 ± 0.05 nmol/kg, $n = 7$) is similar to the NADW SFe at the South Atlantic site (0.33 ± 0.05 nmol/kg, $n = 4$). However, the CFe in NADW decreases from 0.32 ± 0.12 nmol/kg (1 SD, $n = 6$) to 0.15 ± 0.05 nmol/kg (1 SD, $n = 4$). Both the measured differences in the DFe and CFe between the North Atlantic sites to South Atlantic site are significant at the 95% confidence level using the t-test and a distribution-free test, the Kolmogorov–Smirnov test (Hollander and Wolfe, 1973).

Using the same approach use for the DFe scavenging residence time (Bergquist and Boyle, 2006), an estimate for the CFe scavenging residence time can also be made assuming no exchange between the CFe and SFe pools. A transit time of NADW from the North Atlantic to the South Atlantic site of ≈56 ± 18 years was used based radiocarbon-derived age estimates for western Atlantic deep water (Broecker and Virgilio, 1991). For the input of Fe from re-mineralization of organic matter along the flow path, it was assumed that 60% of the re-mineralized DFe was released into the CFe fraction (based on the CFe/DFe of the OMZ at the 10°N site). For the dilution factor, it was assumed 20% of the DFe from Antarctic sources diluting NADW was CFe (based on AAIW and AABW from 24.5°S profile). A deep-water scavenging residence time for CFe of 140 ± 100 years was estimated, which is shorter than the similar estimate for DFe indicating that the short residence time of DFe may be driven by preferential scavenging/removal of the colloidal fraction. However, this estimate may not be valid since it is not known how the two fractions of DFe interact.

3.2.4. DFe vesrus CFe

In Fig. 7, all of the DFe and CFe concentration data from the Atlantic are plotted and a positive correlation between DFe and CFe is observed. The y-intercept of the data is at a DFe concentration of ≈0.30 nmol/kg. The CFe fraction of the DFe disappears below DFe concentrations of less than 0.30 nmol/kg, and there is approximately a 1:1 relationship between DFe and CFe above 0.30 nmol/kg ($r^2 = 0.85$). Not only does this relationship illustrate that higher DFe concentrations are usually due to CFe, but also suggests that there may be some control on how high SFe concentrations can reach and/or that CFe exists when SFe reaches a certain concentration. The y-intercept value for SFe of 0.3 nmol/kg is likely not a solubility limit as SFe values greater than 0.3 nmol/kg exist in the data set. Surface water values greater than 0.4 nmol/kg for SFe exist at three stations near the zone of maximum transport of Saharan dust (≈20°N) with one value reaching 0.54 nmol/kg. The general low concentrations of SFe in the surface waters and the narrow range observed in the deep-water of the Atlantic likely reflects the balance of several factors including the input of DFe, the distribution of soluble and colloidal ligands, the kinetics of formation/dissociation of certain Fe species including possibly inorganic Fe colloids, and the shorter residence time of CFe (i.e., preferential loss of CFe).

Unfortunately not much is known about the distribution of organic ligands in the CFe and SFe pool, but it is probable that organic ligands may play a role in establishing the relationship between the two pools of DFe (Wu et al., 2001; Cullen et al., 2006). Only a few studies have investigated Fe binding organic ligands in the colloidal and soluble pools with excess organic ligands being found in both the soluble and colloidal size fractions (Wu et al., 2001; Cullen et al., 2006). Using competitive ligand exchange methods, Cullen et al. (2006), observed differences between the strengths of excess ligands between surface and deep-water with stronger ligands observed in surface water than in deep-water. The results from this study suggested that equilibrium partitioning between colloidal and soluble ligands is partially responsible for the distribution of Fe between the two size classes, but a significant fraction of the colloidal Fe was inert to ligand exchange. How the distribution of these organic ligands plays a role in the distribution of SFe and CFe still remains an open question that needs more exploration.

4. CONCLUSIONS

In the subtropical and tropical Atlantic, variations in DFe are dominated by changing CFe. The surface DFe and CFe followed dust deposition trends more strongly than the SFe, and observed surface maxima in DFe profiles were always associated with maxima in CFe. These observations support arguments by Wu et al. (2001) that atmospheric Fe is preferentially released into the colloidal fraction. Where dust deposition is low and CFe is low to negligible (i.e. the South Atlantic), the residence time of DFe may be longer because of a smaller fraction of CFe.

SFe and CFe depth profiles had distinct profiles both in the upper water column and in deeper waters. SFe concentration distributions and profiles showed little variability in the Atlantic Ocean with slightly lower concentrations of SFe in the upper ocean at some sites (surface water and in the deep pycnoclines of the gyre sites) than the relatively uniform concentrations in deep-water (≈0.3 to 0.4 nmol/kg). This behavior of SFe was also observed at a North Pacific site in Wu et al. (2001). CFe profiles showed significantly more variability. At sites with surface maxima in CFe, the CFe always decreased to negligible levels at depths of 30–80 m either in the mixed layer or below. At two gyre sites (24.5°S and likely the Wu et al. (2001) 35°N site near the Bermuda Rise), the CFe pool remained negligible throughout the deep pycnocline. At the 30°N gyre station, which also had a deep pycnocline, DFe and CFe also remained low throughout the pycnocline with CFe accounting for 30% of the DFe. The low DFe and CFe in the deep pycnoclines of the gyre sites may be due to ventilation with water from higher latitiudes with lower dust input (and thus lower CFe).

In contrast to the gyre sites, the 10°N station was located on the edge of the equatorial system and had a very shallow pycnocline (<250 m). It was the only station that did not have a surface maximum in DFe or CFe, but only in the winter when the mixed layer was deep. DFe increased rapidly within the shallow pycnocline to concentrations >1 nmol/kg associated with an OMZ at depths of 130–1050 m. A majority of the increase in DFe resulted from increasing CFe. The elevated DFe and CFe in the OMZ is likely due to re-mineralization of organic matter under the high-productivity equatorial upwelling region and poor ventilation of this water (Siedler and Onken, 1996; Brea et al., 2004; Stramma et al., 2005). Under the more stratified summer conditions, the 10°N site had a surface maximum followed by a minimum from 50 to 100 m in the CFe. We have not established the mechanisms that cause the shallow minima in CFe, but it may be due to (1) transient atmospheric deposition and downward mixing and/or (2) a Fe sink within the euphotic zone such as particle scavenging and/or a biological uptake mechanism.

Deep-water DFe and CFe concentrations vary with water mass and with the source, age, and path of the water masses. DFe concentrations in NADW decrease by 30% from the North Atlantic to South Atlantic with most of the decrease associated with the colloidal pool. Despite the loss in CFe, the NADW CFe and DFe concentrations at 24.5°S are still higher than the concentrations in the Antarctic derived water masses (AAIW and AABW). DFe concentrations in AAIW and AABW/LCPDW are low (≈0.4 nmol/kg), which is consistent with observations of DFe in the Southern Ocean. Approximately 20% of the DFe in the Antarctic water masses is CFe and likely reflects their low-dust and low DFe source region.

SFe in the Atlantic shows little variability, therefore most of the variability observed is due to CFe. This was illustrated by a near 1:1 correlation between DFe and CFe above a DFe concentration of ≈0.3 nmol/kg. If one assumes there is no exchange from the SFe pool to the CFe pool, then a scavenging residence time for CFe was estimated from the decrease in NADW from the North Atlantic to South Atlantic (140 ± 100 years). This is shorter than a similar estimate for DFe (270 ± 140 years), and suggests that the short residence time of DFe is driven by preferential loss of the colloidal fraction.

ACKNOWLEDGMENTS

This research was supported by NSF Grants OCE-0002273 and OCE-99871442. B. Bergquist was funded by the National Physical Science Foundation, Lawrence Livermore National Laboratory, and the Education Office of Woods Hole Oceanographic Institution. The authors are grateful for the suggestions by three anonymous reviewers that improved this manuscript. We thank Richard Kayser for all his time and work preparing and maintaining MITESS. We thank our colleagues in the MANTRA Biocomplexity project for all their help at sea and useful discussions. Special thanks go to M. Neumann and M. Erickson for assisting in MITESS deployment and recovery at sea and to Ron Siefert and Ying Chen for aerosol collection and analysis. We thank the officers and crews of the R/V Knorr, R/V Seward Johnson, and R/V Endeavor.

APPENDIX A

Surface Transect Data

Cruise	Date	Lat. (°N, neg. °S)	Long. (°W)	DFe[a] (nmol/kg)	1 SD[c]	*n*	SFe[b] (nmol/kg)	1 SD[c]	*n*
SJ0101	1/14/01	30	45.3	0.48	0.04	2	0.37	0.07	2
January 2001	1/16/01	26.2	45.0	0.49	0.05	3			
	1/17/01	25.1	44.7	?1.13	0.07	2			
	1/17/01	24	45.0	0.73	0.03	2			
	1/17/01	23	45.0	0.79	0.06	4	0.40	0.08	1
	1/18/01	21.7	45.0	0.89	0.02	2			
	1/18/01	20.5	45.0	0.84	0.05	4			
	1/18/01	18.4	45.0	0.68	0.04	3			
	1/19/01	18	45.0	0.63	0.04	4	0.51	0.03	4
	1/19/01	15.8	45.0	0.65	0.04	6	0.42	0.04	2
	1/20/01	14.4	45.0	?0.91	0.05	3			
	1/20/01	12.3	45.0	0.30	0.04	3			
	1/20/01	11.6	45.0	0.43	0.01	2	?0.74	0.02	2
	1/20/01	10.6	45.0	0.37	0.06	3			
	1/21/01	10.2	45.0	0.54	0.06	6	0.22	0.08	3
En367	3/1/02	11.4	56.4	0.55	0.04	3			
March 2002	3/2/02	10.5	54.5	0.71	0.03	3	0.31	0.05	2
	3/4/02	8.1	50.9	?1.42	0.02	2	0.14	0.05	3
	3/4/02	7.0	49.5	0.50	0.01	2	0.36	0.03	3
	3/5/02	6.2	48.4	0.53	0.02	3	0.27	0.06	2
	3/6/02	4.3	45.6	0.50	0.03	3	0.21	0.03	3
	3/6/02	3.34	44.5	0.62	0.03	3	0.21	0.02	8
	3/7/02	3.1	43.8	0.71	0.03	3			
	3/8/02	2.1	41.5	0.62	0.01	3	?1.54	0.20	3
	3/9/02	0.6	37.8	?1.69	0.00	1	0.36	0.05	3
	3/9/02	−0.5	35.0	0.59	0.00	3			
	3/9/02	−0.5	35.0	0.51	0.01	3	0.21	0.03	3
	3/12/02	−7.4	31.4	0.24	0.06	3			
	3/12/02	−8.5	31.5	0.28	0.02	3			
	3/14/02	−11.7	32.2	0.35	0.04	3	0.33	0.02	3
	3/13/02	−11.7	32.1	0.26	0.02	2	0.23	0.02	2
	3/14/02	−12.5	32.2	0.24	0.01	2			
	3/15/02	−14.9	32.9	0.28	0.07	4	0.25	0.01	2
	3/15/02	−16.6	33.3	0.26	0.03	3	0.28	0.02	2
	3/16/02	−19.0	34.0	0.24	0.03	2			
	3/16/02	−19.2	34.1	0.22	0.03	2	0.26	0.01	3

Appendix A (*continued*)

Cruise	Date	Lat. (°N, neg. °S)	Long. (°W)	DFe[a] (nmol/kg)	1 SD[c]	*n*	SFe[b] (nmol/kg)	1 SD[c]	*n*
	3/17/02	−21.9	35.5	0.34	0.02	3	0.36	0.05	3
	3/17/02	−23.5	36.4	0.38	0.03	3	0.31	0.03	3
	3/18/02	−24.1	36.7	0.35	0.05	3	0.23	0.02	3

?, Sample data is suspected to be contamination and is not considered in figures and discussion.

[a] DFe is the Fe that passes through a 0.4 μm filter.

[b] SFe is the Fe that passes through a 0.02 μm filter.

[c] 1 SD is the standard deviation of sample replicates.

APPENDIX B

Water Profile Data

Cruise-St	Date	Lat.	Long.	Depth (m)	DFe[a] (nmol/kg)	1 SD[c]	*n*	SFe[b] (nmol/kg)	1 SD[c]	*n*
30°N profile SJ0101, January 2001	1/14/01	30.0°N	45.3°W	0.2	0.68	0.04	3	0.34	0.02	3
				41	0.58	0.03	3	0.34	0.05	1
				63	0.39	0.01	3	0.32	0.03	3
				77	0.37	0.01	2	0.33	0.05	3
				165	0.41	0.02	2	0.28	0.01	3
				200	?0.63	0.04	3	0.28	0.05	3
				250	0.42	0.03	3	0.33	0.03	3
				375	?1.19	0.08	3	0.35	0.01	3
				450	0.41	0.01	2	?0.48	0.03	3
				525	?0.74	0.03	3	0.36	0.03	2
				850	0.55	0.04	3	0.42	0.01	3
				950	0.57	0.02	3	0.41	0.00	2
				1050	0.51	0.01	2	0.35	0.01	2
10°N profile SJ0101, January 2001	1/21/01	10.2°N	45.0°W	0	0.54	0.06	6	0.22	0.08	3
				30	0.68	0.01	2	0.35	0.11	3
				130	1.08	0.08	4	?2.98	0.03	2
				165	0.98	0.04	2	0.33	0.17	2
				200	1.19	0.16	3	0.41	0.11	3
				250	1.05	0.01	2	0.46	0.01	3
				375	1.19	0.02	2	0.41	0.05	4
				525	1.11	0.03	2	0.45	0.02	2
				725	1.06	0.11	2	0.31	0.08	3
				850	1.16	0.03	4	0.40	0.10	3
				1050	1.01	0.07	3	0.46	0.02	2
				1250	0.98	0.10	3	0.42	0.06	2
				1500	0.77	0.02	3	0.58	0.10	3
				1750	0.70	0.13	6	0.45	0.02	3
				3400	0.86	0.05	4	0.36	0.02	2
				4200	0.63	0.13	2	0.42	0.05	2
30°N profile Kn162, July 2001,	7/2/01	30.0°N	45.0°W	0	0.51	0.04	3			
				2	0.49	0.03	2	?0.60	0.01	3
				2	0.51	0.02	3			
				4	0.54	0.03	2	0.43	0.03	3
				6	0.56	0.03	3	0.29	0.02	2
				8	0.47	0.02	3	0.33	0.01	2
				8	0.44	0.02	3			
				11	0.44	0.02	3	0.34	0.02	2
				14	0.46	0.02	3	0.48	0.03	3
				17	0.49	0.01	2	?0.68	0.03	3
				19	0.45	0.03	2	0.23	0.06	2
				30	0.42	0.02	3	0.41	0.03	4
				39	0.42	0.03	4	0.39	0.02	3
				79	0.36	0.02	3	0.32	0.03	3
				79	0.37	0.05	2			
				197	0.44	0.05	2	?0.49	0.00	2
				197	0.42	0.03	2			

(*continued on next page*)

Appendix B (*continued*)

Cruise-St	Date	Lat.	Long.	Depth (m)	DFe[a] (nmol/kg)	1 SD[c]	*n*	SFe[b] (nmol/kg)	1 SD[c]	*n*
10°N profile Kn162, July 2001	7/12/01	10.1°N	45.5°W	0	0.60	0.03	3	0.41	0.05	2
				2	0.71	0.04	3	0.37	0.04	3
				5	0.59	0.03	3	0.40	0.05	3
				7	0.55	0.02	3	0.65	0.03	2
				10	0.48	0.05	3	0.40	0.05	3
				13	0.45	0.02	3	0.34	0.01	2
				16	0.51	0.00	2	?2.96	0.27	3
				19	0.62	0.04	3	0.36	0.12	3
				22	0.56	0.01	3	0.42	0.00	2
				25	0.53	0.02	2	0.44	0.01	2
				28	0.55	0.04	3	0.45	0.05	3
				49	0.40	0.04	3	0.44	0.03	3
				79	0.37	0.03	3	0.41	0.05	3
				148	0.54	0.03	3	0.40	0.01	3
				198	0.75	0.04	3	0.82	0.02	3
24.5°S profile En367, Mar. 2002	3/18/02	24.5°S	37.0°W	1	0.36	0.05	3	0.24	0.02	3
				18	0.39	0.02	2	0.30	0.01	3
				69	0.24	0.04	2	0.28	0.02	2
				113	0.29	0.02	3	0.26	0.05	3
				239	?0.50	0.01	2	?0.61	0.01	2
				394	0.26	0.04	3	0.26	0.04	2
				544	0.28	0.00	2	?0.46	0.05	1
				709	0.37	0.03	2	0.31	0.02	3
				841	0.39	0.03	3	0.31	0.01	3
				985	0.39	0.01	3	?0.45	0.03	3
				1181	0.38	0.05	1	0.35	0.03	3
				1366	0.45	0.03	3	0.32	0.03	3
				1649	0.43	0.04	2	0.38	0.05	3
				1787	0.45	0.01	3	?3.83	0.29	2
				1920	0.45	0.02	2	?0.55	0.05	2
				2198	0.46	0.03	3	0.33	0.01	3
				2494	0.49	0.05	2	0.30	0.00	2
				2676	0.50	0.02	2	0.40	0.01	3
				3051	0.48	0.02	3	0.35	0.01	3
				3308	0.49	0.02	3	0.27	0.02	2
				3556	0.41	0.02	3	?0.48	0.05	1
				3806	0.43	0.03	3	0.29	0.04	3
				3905	0.43	0.02	3			
				4029	0.41	0.02	2	0.35	0.01	3

?, Sample data is suspected to be contamination and is not considered in figures and discussion.

[a] DFe is the Fe that passes through a 0.4 µm filter.

[b] SFe is the Fe that passes through a 0.02 µm filter.

[c] 1 SD is the standard deviation of sample replicates.

REFERENCES

Barbeau K., and Moffett J. W. (1998) Dissolution of iron oxides by phagotropic protists: using a novel method to quantify reaction rates. *Environ. Sci. Technol.* **32**, 2969–2975.

Barbeau K., and Moffett J. W. (2000) Laboratory and field studies of colloidal iron oxide dissolution as mediated by phagotrophy and photolysis. *Limnol. Oceanogr.* **45**, 827–835.

Barbeau K., Moffett J. W., Caron M. A., Croot P. L., and Erdner D. L. (1996) Role of protozoan grazing in relieving iron limitation of phytoplankton. *Nature* **380**, 61–64.

Bell J., Betts J., and Boyle E. A. (2002) MITESS: a moored in-situ trace element serial sampler for deep-sea moorings. *Deep-Sea Res. Part I* **49**, 2103–2118.

Bergquist, B. A. (2004) The Marine Geochemistry of Iron and Iron Isotopes, Ph.D. thesis, Massachusetts Institute of Technology and Woods Hole Oceanographic Institution Joint Program in Oceanography.

Bergquist B. A., and Boyle E. A. (2006) Dissolved iron in the tropical and subtropical Atlantic Ocean. *Global Biogeochem. Cycles* **20**, GB1015.

Boyd P. W., Law C. S., Wong C. S., Nojiri Y., Tsuda A., Levasseur M., Takeda S., Rivkin R., Harrison P. J., Strzepek R., Gower J., McKay R. M., Abraham E., Arychuk M., Barwell-Clarke J., Crawford W., Crawford D., Hale M., Harada K., Johnson K., Kiyosawa H., Kudo I., Marchetti A., Miller W., Needoba J., Nishioka J., Ogawa H., Page J., Robert M., Saito H., Sastri A., Sherry N., Soutar T., Sutherland N., Taira Y., Whitney F., Wong S. K. E., and Yoshimura T. (2004) The decline and fate of an iron-induced subarctic phytoplankton bloom. *Nature* **428**, 549–553.

Boyd P. W., Watson A. J., Law C. S., Abraham E. R., Trull T., Murdoch R., Bakker D. C. E., Bowie A. R., Buesseler K. O., Chang H., Charette M., and Croot P., et al. (2000) A mesoscale phytoplankton bloom in the polar Southern Ocean stimulated by iron fertilization. *Nature* **407**, 695–702.

Boyle E. A., Bergquist B. A., Kayser R., and Mahowald N. (2005) Iron, manganese, and lead at Hawaii Ocean Time Series Station ALOHA: temporal variability and an intermediate water hydrothermal plum. *Geochim. Cosmochim. Acta* **69**, 933–952.

Brea S., Alverez-Salgado X. A., Alvarez M., Perez F. F., Memery L., Mercier H., and Messias M. J. (2004) Nutrient mineralization rates and ratios in the eastern South Atlantic. *J. Geophys. Res.* **109**, C05030.

Broecker W. S., and Virgilio A. (1991) Radiocarbon age of waters in the deep Atlantic revisited. *Geophys. Res. Lett.* **18**, 1–3.

Bruland K. W., Orians K. J., and Cowen J. P. (1994) Reactive trace metals in the stratified central North Pacific. *Geochim. Cosmochim. Acta* **58**, 3171–3182.

Chen M., Dei R. C. H., Wang W., and Guo L. (2003) Marine diatom uptake of iron bound with natural colloids of different origins. *Mar. Chem.* **81**, 177–189.

Chen M., and Wang W. X. (2001) Bioavailability of natural colloidal Fe to marine plankton: influence of colloidal size and aging. *Limnol. Oceanogr.* **46**, 1956–1960.

Chen Y., and Siefert R. (2004) Seasonal and spatial distributions of dry deposition fluxes of atmospheric total and labile iron over the tropical and sub-tropical North Atlantic Ocean. *J. Geophys. Res. [Atmos.]* **109**, 1–18. Art. No. D09305.

Coale K. H., Johnson K. S., Chavez F. P., Buesseler K. O., Barber R. T., Brzezinski M. A., Cochlan W. P., Millero F. J., Falkowski P. G., Bauer J. E., Wanninkhof R. H., Kudela R. M., Altabet M. A., Hales B. E., Takahashi T., Landry M. R., Bidigare R. R., Wang X. J., Chase Z., Strutton P. G., Friederich G. E., Gorbunov M. Y., Lance V. P., Hilting A. K., Hiscock M. R., Demarest M., Hiscock W. T., Sullivan K. F., Tanner S. J., Gordon R. M., Hunter C. N., Elrod V. A., Fitzwater S. E., Jones J. L., Tozzi S., Koblizek M., Roberts A. E., Herndon J., Brewster J., Ladizinsky N., Smith G., Cooper D., Timothy D., Brown S. L., Selph K. E., Sheridan C. C., Twining B. S., and Johnson Z. I. (2004) Southern ocean iron enrichment experiment: carbon cycling in high- and low-Si waters. *Science* **304**, 408–414.

Coale K. H., Johnson K. S., Fitzwater S. E., Gordon R. M., Tanner S., Chavez F. P., Ferioli L., Sakamoto C., Rogers P., Millero F., Steinberg P., Nightingale P., Cooper D., Cochlan W. P., Landry M. R., Constantinou J., Rollwagen G., Trasvina A., and Kudela R. (1996) A massive phytoplankton bloom induced by an ecosystem-scale iron fertilization experiment in the equatorial Pacific Ocean. *Nature* **383**, 495–501.

Cullen J. T., Bergquist B. A., and Moffett J. W. (2006) Thermodynamic characterization of the partitioning of iron between soluble and colloidal species in the Atlantic Ocean. *Mar. Chem.* **98**, 295–303.

de Baar H. J. W., de Jong J. T. M., Bakker D. C. E., Loscher B. M., Veth C., Bathmann U., and Smetacek V. (1995) The importance of iron for plankton blooms and carbon dioxide drawdown in the Southern Ocean. *Nature* **373**, 412–415.

Duce R. A., and Tindale N. W. (1991) Atmospheric transport of iron and its deposition in the ocean. *Limnol. Oceanogr.* **36**, 1715–1726.

Falkowski P. G. (1998) Evolution of the nitrogen cycle and its influence on the biological sequestration of CO_2 in the ocean. *Nature* **387**, 272–275.

Fung I. Y., Meyn S. K., Tegen I., Doney S. C., John J. G., and Bishop K. B. (2000) Iron supply and demand in the upper ocean. *Global Biogeochem. Cycles* **14**, 281–295.

Gao Y., Kaufman Y. J., Tanre D., Kolber D., and Falkowski P. G. (2001) Seasonal distributions of aeolian iron fluxes to the global ocean. *Geophys. Res. Lett.* **28**, 29–32.

Gledhill M., and van den Berg C. M. G. (1994) Determination of complexation of iron(III) with natural organic complexing ligands in seawater using cathodic stripping voltammetry. *Mar. Chem.* **47**, 41–54.

Gregg W. W., Ginoux P., Schopf P. S., and Casey N. W. (2003) Phytoplankton and iron: validation of a global three-dimensional ocean biogeochemical model. *Deep-Sea Res. Part II* **50**, 3143–3169.

Hollander M., and Wolfe D. A. (1973) *Nonparametric Statistical Methods*. John Wiley & Sons.

Hutchins D. A., and Bruland K. W. (1998) Iron-limited diatom growth and Si: N uptake ratios in a coastal upwelling regime. *Nature* **393**, 561–564.

Hutchins D. A., Witter A. E., Butler A., and Luther G. W. (1999) Competition among marine phytoplankton for different chelated iron species. *Nature* **400**, 858–861.

Karl D. M., Letelier R. D., Tupas L., Dore J., Christian J., and Hebel D. (1997) The role of nitrogen fixation in biogeochemical cycling in the subtropical North Pacific Ocean. *Nature* **388**, 533–537.

Kumar N., Anderson R. F., Mortlock R. A., Froelich P. N., Kubik P., Dittrich-Hannon B., and Suter M. (1995) Increased biological productivity and export production in the glacial Southern Ocean. *Nature* **378**, 675–680.

Letelier R. M., and Karl D. M. (1996) The role of *Trichodesmium* spp. in the productivity of the subtropical North Pacific. *Mar. Ecol. Prog. Ser.* **57**, 173–179.

Loscher B. M., de Baar H. J. W., de Jong J. T. M., Veth C., and Dehairs F. (1997) The distribution of Fe in the Antarctic circumpolar current. *Deep-Sea Res. Part II* **44**, 143–187.

Luther G. W. I., and Wu J. (1997) What controls dissolved iron concentrations in the world ocean?—a comment. *Mar. Chem.* **57**, 173–179.

Mahowald N., Kohfeld K., Hansson M., Balkanski Y., Harrison S. P., Prentice I. C., Schulz M., and Rodhe H. (1999) Dust sources and deposition during the last glacial maximum and current climate: a comparison of model results with paleodata from ice cores and marine sediments. *J. Geophys. Res.* **104**, 15895–15916.

Martin J. H., Coale K. H., Johnson K. S., Fitzwater S. E., Gordon R. M., Tanner S. J., Hunter C. N., Elrod V. A., Nowicki J. L., Coely T. L., Barber R. T., Lindley S., Watson A. J., van Scoy K., Law C. S., Liddicoat M. I., Ling R., Stanton T., Stockel J., Collins C., Anderson A., Bidigare R., Ondrusek M., Latasa M., Millero F. J., Lee K., Yao W., Zhang J. Z., Friederich G., Sakamoto C., Chevez F., Buck K., Kolber Z., Greene R., Falkowski P., Chisholm S. W., Hoge F., Swift R., Yungel J., Turner S., Nightingale P., Hatton A., Liss P., and Tindale N. W. (1994) Testing the iron hypothesis in ecosystems of the equatorial Pacific Ocean. *Nature* **371**, 123–129.

Martin J. H., and Fitzwater S. E. (1988) Iron deficiency limits phytoplankton growth in the north-east Pacific subarctic. *Nature* **331**, 341–343.

Martin J. H., Fitzwater S. E., and Gordon R. M. (1990a) Iron deficiency limits phytoplankton growth in Antarctic waters. *Global Biogeochem. Cycles* **4**, 5–12.

Martin J. H., Gordon R. M., and Fitzwater S. E. (1990b) Iron in Antarctic waters. *Nature* **345**, 156–158.

Measures C. I. (1995) The distribution of Al in the IOC stations of the eastern Atlantic between 30-degrees-S and 34-degrees-N. *Mar. Chem.* **49**, 267–281.

Michaels A. F., Olson D., Sarmiento J. L., Ammerman J. W., Fanning K., Jahnke R., Knap A. H., Lipschultz F., and Prospero J. M. (1996) Inputs, losses and transformation of nitrogen and phosphorus in the pelagic North Atlantic Ocean. *Biogeochemistry* **35**, 181–226.

Nordwell L. M., and Price N. B. (2001) Direct use of inorganic colloidal iron by marine mixotrophic phytoplankton. *Limnol. Oceanogr.* **46**, 765–777.

Powell R., and Donat J. (2001) Organic complexation and speciation of iron in the South and Equatorial Atlantic. *Deep-Sea Res. Part II* **48**, 2877–2893.

Prospero, J. M. (1996) The atmospheric transport of particles to the ocean. In *Particle Flux in the Ocean* (eds. V. Ittekkott, P. Schafer, S. Honjo, and P.J. Depestris). Vol. SCOPE Rep. 57. John Wiley, pp. 19–52.

Rue E. L., and Bruland K. W. (1995) Complexation of iron(III) by natural ligands in the central North Pacific as determined by a new competitive ligand equilibrium/adsorptive cathodic stripping voltammetric method. *Mar. Chem.* **50**, 117–138.

Rueter J. G., and Ades D. R. (1987) The role of iron nutrition in photosynthesis and nitrogen assimilation in Scenedesmus quadeicauda (Chlorophyceae). *J. Phycol.* **23**, 452–457.

Siedler G., and Onken R. (1996) Eastern recirculation. In *The Warm Water Sphere of the North Atlantic Ocean*, (ed. W. Krauss), pp. 339–364. Gebruder Borntrager, Berlin.

Stramma L., Huttle S., and Schafstall J. (2005) Water masses and currents in the upper tropical northeast Atlantic off of northwest Africa. *J. Geophys. Res.* **110**, C12006.

Tchernia P. (1980) *Descriptive Regional Oceanography*. Pergamon Press.

Vink S., Boyle E. A., Measures C. I., and Yuan J. (2000) Automated high resolution determination of the trace elements iron and aluminum in the surface ocean using towed fish coupled to a flow injection analysis. *Deep-Sea Res. Part I* **47**, 1141–1156.

Vink S., and Measures C. I. (2001) The role of dust deposition in determining surface water distributions of Al and Fe in the South West Atlantic. *Deep-Sea Res. Part II* **48**, 2787–2809.

Witter A. E., and Luther G. W. (1998) Variation in Fe-organic complexation with depth in the Northwestern Atlantic Ocean as determined using a kinetic approach. *Mar. Chem.*, 241–258.

Wu J., and Boyle E. A. (1998) Determination of iron in seawater by high resolution isotope dilution inductively coupled plasma mass spectrometry after $Mg(OH)_2$ coprecipitation. *Anal. Chim. Acta* **367**, 183–191.

Wu J., and Boyle E. A. (2002) Iron in the Sargasso Sea: implications for the processes controlling dissolved Fe distribution in the ocean. *Global Biogeochem. Cycles* **16**, 1086–1094.

Wu J., Boyle E. A., Sunda W., and Wen L. (2001) Soluble and colloidal iron in the oligotrophic North Atlantic and North Pacific. *Science* **293**, 847–849.

Wu J., and Luther G. W. I. (1995) Complexation of iron(III) by natural organic ligands in the Northwest Atlantic Ocean by competitive ligand equilibration method and a kinetic approach. *Mar. Chem.* **50**, 159–177.

Associate editor: Robert H. Byrne